MRS Advances © 2017 Materials Research Society
DOI: 10.1557/adv.2017.443

Synthesis and characterization of CeO_2 nanoparticles on porous carbon for Li-ion battery

Hoejin Kim[1], Mohammad Arif Ishtiaque Shuvo[1], Hasanul Karim[1], Juan C. Noveron[2], Tzu-liang Tseng[3], and Yirong Lin[1]

[1]Department of Mechanical Engineering, University of Texas at El Paso, El Paso, TX 79968, USA.
[2]Department of Chemistry, University of Texas at El Paso, El Paso, TX 79968, USA.
[3]Department of Industrial, Systems, and Manufacturing, University of Texas at El Paso, El Paso, TX 79968, USA.

ABSTRACT

Carbon based materials have long been investigated as anodes for lithium ion batteries. Among these materials, porous carbon holds several advantages such as high stability, high specific surface area, and excellent cycling capability. To further enhance the energy storage performance, ceramic nanomaterials have been combined with carbon based materials as hybrid anodes for enhanced specific capacity. The use of metal oxide ceramic nanomaterials could enhance the surface electrochemical reactivity thus leads to the increasing of capacity retention at higher number of cycles. In this research, we synthesized ceria (CeO_2) nano-particles on porous carbon to form inorganic-organic hybrid composites as an anode material for Li-ion battery. The high redox potential of ceria is expected to increase the specific capacity and energy density of the system. The electrochemical performance was determined by a battery analyzer. It is observed that the specific capacity could be improved by 77% using hybrid composites anode. The material morphology, crystal structure, and thermal stability were characterized by Scanning Electron Microscopy (SEM), Transmission Electron Microscopy (TEM), X-Ray Diffraction (XRD), and Thermogravimetric Analysis (TGA).

1. INTRODUCTION

The ever-increasing demand for portable electronic devices, transportation, and energy storage for intermittent renewable energy sources (e.g., solar and wind powers) is the driving force behind the technological improvements of electrochemical energy storage devices such as batteries [1-3], capacitors [4-6], and super-capacitors [7]. Lithium-ion battery (LIB) is widely considered as the technology of choice due to its high energy density, lightweight and flexible design, and long lifespan [2, 8]. The route towards innovating future LIB depends on either synthesizing novel electrode materials or formulating a unique electrolyte with higher voltage window. Carbon based materials with different textures, morphologies, and crystallinities have received much attention for anode application in LIBs due to its abundance, thermal and chemical stability, and low cost. Presently, graphite is widely used as anode materials for the commercial productions of LIBs, however, lithium storage capacity of graphite is limited. The multilayer nature of graphite materials limits Li-ion diffusion, resulting in low charge-discharge rate performance for the battery [1].

Therefore, much effort has been given to the exploration of amorphous porous carbon materials in order to increase the lithium storage capacity. Existence of micro-pores and macro-pores in carbon based materials exerts significant effect on their electronic structure and performance which helps in LIB performance. Ji et al. showed that porous carbon nano-fibers have better reversible capacity and cycling performance than conventional graphite anode due to the porous structure that facilitates ion transportation [9]. Juan et al. reported that porous carbon

structure is an excellent candidate for anode materials for high power density LIB [10]. In addition, various nano-materials of metal oxides have been used as anode materials for LIB [9, 11, 12]. Hybrid nanostructure electrodes, which interconnect nano-structured electrode materials with conductive additive nano-phases, are another way of improving Li-ion insertion properties [9, 13, 14]. For example, hybrid nanostructures such as Mn_3O_4-graphene hybrids or $LiFePO_4$-RuO_2 nano-composites, combined with conventional carbon additives (e.g., acetylene black), have demonstrated an increased Li-ion insertion/extraction capacity in hybrid electrodes at high charge/discharge rates [11, 15]. Homogenously dispersed Fe_3O_4 nano-cystals in porous carbon foam exhibited a significantly improved coulombic efficiency and cyclic stability for LIB [3].

Cerium oxide (CeO_2) is a rare earth element oxide that has a high oxygen storage capacity, high electrical conductivity, diffusivity, and high thermal stability [16, 17]. It offers high potential as an anode material for LIB due to its fast transformation between Ce (III) and Ce (IV) oxalates which have relatively low decomposition temperature in air, good structural stability and relatively low cost [18].

In this paper, we demonstrated a highly efficient and low cost synthesize method of fabricating a hybrid anode structure using porous carbon (PC) and CeO_2 nano-particles. A simple hydrothermal method was utilized to obtain CeO_2 nano-particles on porous carbon. The obtained porous carbon/CeO_2 nano-particles (PC-CON) hybrid electrode material was compared with porous carbon (PC). The PC-CON hybrid has shown higher reversible capacity and rate capacity than PC when used in LIB as an anode material. This simple hybrid anode material synthesis method has the potential to be utilized for large-scale anode material production for LIBs.

2. EXPERIMENTAL DETAILS

2.1 Synthesis of Porous Carbon/Cerium Oxide Nano-particle (PC/CON) hybrid materials

The PC/CON hybrid synthesis is a one-step hydrothermal method [18]. At first, 100mg of porous carbon (ACS Material, LLC) was dispersed in 200mL of deionized water (DI) water. Then 150mL of 0.02M Ammonium Cerium Nitrate $(NH4)_2Ce(NO_3)_6$ was added to the solution and sonicated (Branson Sonifier 450) for 45 minutes. The mixture was then separated by centrifugation. At this stage $Ce(OH)_4$ was formed into the pores and on the surfaces of the porous carbon [18]. Then the product was mixed with 100mL 5M NaOH solution and transferred into a Teflon-lined autoclave. After heating the mixture for 45 hours at 180°C, the solution was separated by centrifugation, washed with DI water for three times. Then the remnant was dried at 70°C over night. At last the product was heated at 450°C in Argon for 2 hours [19, 20]. Figure 1 shows the schematic view of the PC-CON synthesis process.

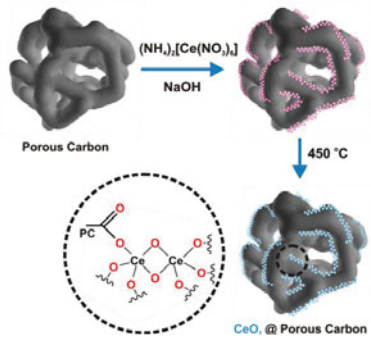

Figure 1. Schematic of CeO_2 synthesis on Porous Carbon.

2.2 Anode Preparation

For making anodes of both PC and PC-CON electrodes, polyvinylidene fluoride (PVDF, MTI corp., purity ≥99.5%) was used as a binding material. PVDF was dissolved in N-Methyl-2-pyrrolidone (NMP, MTI corp., purity ≥99.5%) at a 1:2.5 weight ratio by heating at 80 °C. Later 80 wt. % active material and 10 wt. % activated carbon were dispersed in 10 wt. % PVDF with excess NMP to prepare homogenous slurry using a homogenizer (Fisher Scientific, Model 125). Then the slurry was coated on copper foil and dried at 100°C on a hot plate. Next, a precision disc cutter from MTI Corporation was used to cut anodes with 13 mm in diameter and uniformly distributed 110-130 µm in thickness all over the electrode. Later the anodes were kept overnight in a vacuum oven at room temperature. The whole anode preparation process is schematically shown in Figure 2.

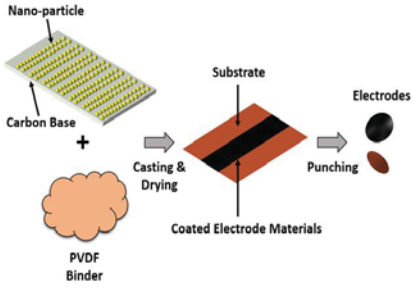

Figure 2. Schematic of the anode preparation.

Coin cells (CR 2032) were assembled using either PC anodes or PC-CON anodes inside an Argon filled glovebox (Unilab, MBraun). Oxygen and moisture level were kept less than 0.1 ppm inside the glovebox. One molar LiPF6 in ethylene carbonate (EC), dimethyl carbonate (DMC), and diethyl carbonate (DEC) organic solvent at 1:1:1 volume ratio was used as electrolyte as received (MTI corp.). Celgard 2500 was used as the separator. A cross-sectional view for coin cell assembly is shown in Figure 3.

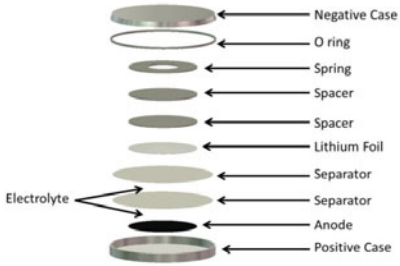

Figure 3. Cross sectional view of coin cell assembly.

3. RESULTS AND DISCUSSION

Scanning Electron Microscopy (SEM) and Transmission Electron Microscopy (TEM) were used to determine size and morphology of PC-CON hybrids as shown in Figure 4. As indicated by the figure, CeO_2 particles were formed on the surfaces and nooks of the porous carbon. The nano-particles had a diameter between 6 to 8 nm. Clear lattice fringes were observed by HRTEM image which confirms the formation of crystalline particles during the hydrothermal reaction.

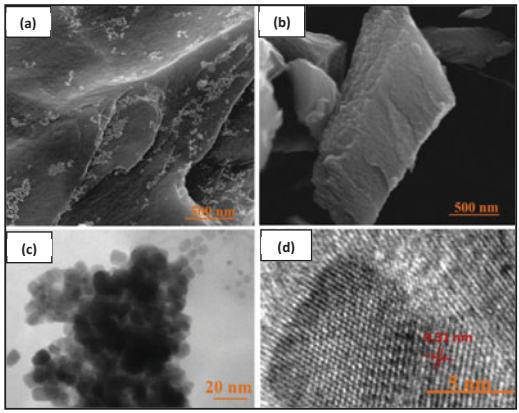

Figure 4. (a) SEM image of CeO_2 nanoparticles on porous carbon, (b) SEM image of porous carbon, (c) TEM image of CeO_2 nanoparticles, (d) HRTEM image of CeO_2 nanoparticles.

The crystal structures of the PC-CON hybrid before and after heat treatment were determined utilizing a Bruker D8 Discover XRD using Cu Kα radiation (Figure 5). The precursor sample shows very weak crystal peaks, indicating more amorphous nature, whereas the sample after heat treatment exhibit diffraction peaks that correspond to (111), (200), (220), (311), and (222) planes of a cubic fluorite structure CeO_2 (space group: Fm3m), which is in agreement with the JCPDS file for CeO_2 (JCPDS 34-0394). It is shown that the reflection peaks become sharper and narrower after heat treatment, indicating that the crystal grows, and the crystallinity of CeO_2 becomes better defined. The values of lattice parameters *a* calculated from the XRD spectra before and after heat treatment are 0.534 and 0.544 nm

respectively. It is noted that the values of lattice parameter *a* for the sample before heat treatment is lower than the heat-treated sample. Our results are in agreement with those of Leoni et al., who reported that the lattice parameter of nano-crystalline CeO_2 powder changes as a function of temperature due to enhanced crystallinity [21]. No extra peaks corresponding to any other secondary phases were observed.

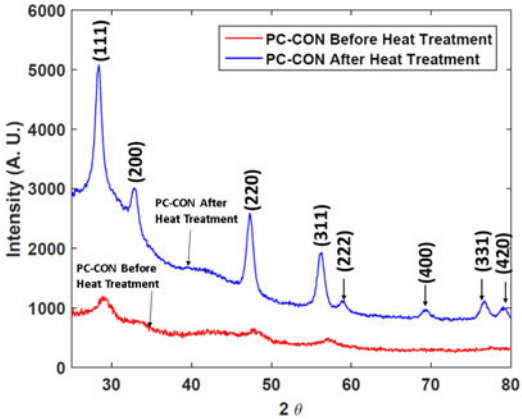

Figure 5. XRD results for PC-CON before and after heat treatment.

Thermogravimetric analysis (TGA) was performed to quantify the weight percentage of CeO_2 nanoparticles present in the PC-CON sample using TG 209 F1 Iris. The ramp rate was set to 20ºC/minute up to 1000ºC in presence of air and the temperature was kept at 1000ºC for 30 minutes. The TGA profile for PC-CON sample presents a sharp weight loss at around 350ºC and accompanied by a heat release which can be observed in the temperature profile. Similarly, the TGA profile for PC shows a sharp weight loss around 500 ºC associated with a heat release (exothermal) due to onset of carbon burnout. Due to the presence of air, all porous carbon started to oxidize at this point and during the dwell time all porous carbon was oxidized and burnt away leaving only CeO_2 particles remaining. It is shown in Figure 6 that the weight percentage of CeO_2 particle is around 44.0 wt. % of PC-CON composites. The TGA profile for PC sample presents a sharp weight loss at around 500ºC and no traces of porous carbon were found after the heating cycle, indicating a 100% burnt out of carbon. Note that the low carbon oxidization onset temperature (350°C instead of 500°C) of the PC-CON is caused by the oxidization reaction between carbon and CeO_2 [22].

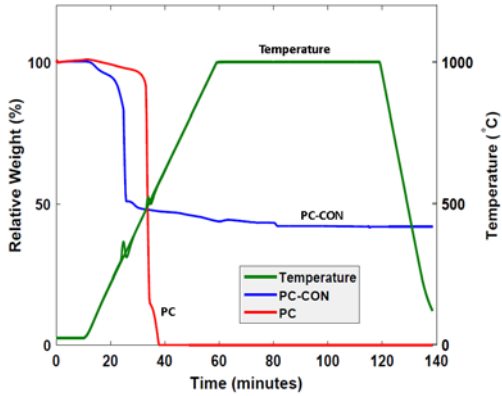

Figure 6. TGA of PC-CON sample.

To evaluate the electrochemical performance of the electrodes, we investigated the Li-ion insertion/extraction properties in PC and PC-CON hybrid materials using MTI eight-channel battery analyzer. Figure 7 (a) and (b) show the galvanostatic charge-discharge curves for PC and PC-CON anodes respectively at the voltage window between 0.01 to 2 V in the 1st, 2nd, 10th and 30th cycles. The current density for both electrodes was maintained at 100mA/g for 40 cycles. Note that no obvious voltage plateau was observed for both cases. The significantly high value of capacity in the first discharge is caused largely by the decomposition of the non-aqueous electrolyte and the formation of solid electrolyte interface (SEI) layer on the electro-active materials [22]. This phenomena would be also likely to protect the electrodes partly and improve the stability of cyclic performance [18, 23]. Figure 7 (c) shows the cyclic performance for PC and PC-CON hybrid electrode. As mentioned before, the cycling stability of PC and PC-CON hybrid electrodes were measured at 100mA/g for 40 cycles. For both sample, the specific capacity decreased with the increase of cycle number. The specific capacity of PC anode was 146 mAh/g at 2nd cycle and decreased to 72 mAh/g at 40th cycle. On the contrary, the specific capacity of PC-CON anode was 187 mAh/g at 2nd cycle and decreased to 128 mAh/g at 40th cycle at the same current density. For the 2nd cycle at same current density the specific capacity of PC-CON anode was 28% higher than the PC anode. At the 40th cycle the specific capacity of PC-CON became 77% higher than PC anode. As testing progresses, the performance of PC anode decreased more than the PC-CON anode. It can be concluding that the increment is due to the CeO_2 nano-particles, since all other testing parameters for both batteries are the same.

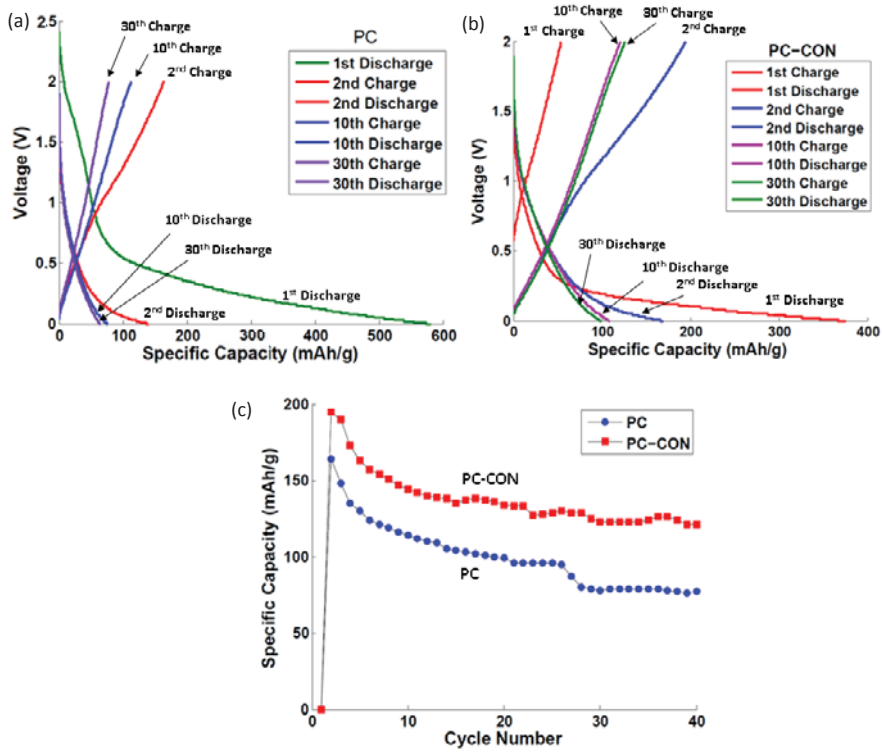

Figure 7. Measurement of capacity and rate capability, (a) charge/discharge curve for PC anode, (b) charge/discharge curve for PC-CON anode, (c) comparison of specific capacity of the two anode materials as a function of cycle number.

Previously it has been found that the lithiation and delithiation process of ceria is a reversible phase transformation between CeO_2 and Ce_2O_3 [24]. The electrochemical process of CeO_2 can be expressed as the following reaction:

$$2\ CeO_2 + 2\ Li^+ + 2e^- \rightarrow Ce_2O_3 + Li_2O$$

The improvement of electrochemical performance PC-CON anode can be attributed to the presence of CeO_2 nano-particles, which provide favorable properties for electrochemical energy conversion in several fronts. The quasi-spherical CeO_2 nano-particles were homogenously dispersed throughout the porous carbon, thus preventing the CeO_2 nano-particles from agglomerating and effectively accommodating the volume change of CeO_2 during charge-discharge process. Therefore, all cerium ions could shift between CeO_2 and Ce_2O_3 under oxidizing and reducing conditions providing more specific capacity to hybrid nano-composites [25]. Finally, PC-CON hybrid electrode provides large electrode/electrolyte contact area and shorter length for Li-ion diffusion with good stability, thus further facilitates the Li-ion transport.

All above-mentioned factors are expected to be responsible for the improved anodes with excellent energy storage capacity, cycling stability, and coulombic efficiency.

4. CONCLUSIONS

Energy storage devices, i.e., battery and super-capacitors, are the bases for green energy solutions. A single step hydrothermal synthesis technique was utilized to synthesize ceria nano-particles on porous carbon to develop a high performance LIB anode material. The growth and presence of ceria was confirmed using SEM, TEM, XRD, and TGA. A 77% improvement of specific capacity was observed from PC-CON hybrid electrode compared to the as purchased PC electrode material in terms of capacitance and cycle stability. The growth of nano-particles has a positive synergistic effect that provides pathways for Li-ion insertion/extraction increasing electrode-electrolyte contact area. This simple method can be utilized in a larger scale production for high-performance LIBs.

ACKNOWLEDGMENTS

This work is supported by the National Science Foundation (NSF) under NSF-PREM Grant No. DMR-1205302. The authors would like to thank Md Tariqul Islam and Dr. Peter H. Cooke, CURRL director at New Mexico State University for TEM facility.

REFERENCES

1. M. A. I. Shuvo, M. A. R. Khan, H. Karim, P. Morton, T. Wilson, and Y. Lin, *ACS appl. mater. & inter.,* 5, 7881-7885 (2013).
2. M. A. I. Shuvo, G. Rodriguez, M. T. Islam, H. Karim, N. Ramabadran, J. C. Noveron*, et al.*, *J. of Appl. Phys.,* 118, 125102 (2015).
3. T. Yoon, C. Chae, Y.-K. Sun, X. Zhao, H. H. Kung, and J. K. Lee, *J. of Mater. Chem.,* 21, 17325-17330 (2011).
4. M. Mendoza, M. A. Rahaman Khan, M. A. Ishtiaque Shuvo, A. Guerrero, and Y. Lin, *ISRN Nano.,* 2012 (2012).
5. M. Rajib, M. A. I. Shuvo, H. Karim, D. Delfin, S. Afrin, and Y. Lin, *Cera. Inter.,* 41, 1807-1813 (2015.)
6. M. Rajib, R. Martinez, M. Shuvo, H. Karim, D. Delfin, S. Afrin*, et al.*, *Inter. J. of Appl. Cera. Tech., (*2015).
7. M. A. I. Shuvo, T.-L. B. Tseng, M. A. R. Khan, H. Karim, P. Morton, D. Delfin*, et al.*, *J. of Appl. Phys.,* 114, 104306 (2013).
8. M. A. I. Shuvo, H. Karim, M. T. Islam, G. Rodriguez, M. I. Nandasiri, A. M. Schwarz*, et al.*, *SPIE Smar. Stru. & Mate.+ Nond. Eval. & Heal. Moni.*, 94390H-94390H-8 (2015).
9. D. Wang, D. Choi, J. Li, Z. Yang, Z. Nie, R. Kou*, et al.*, *ACS nano.,* 3, 907-914 (2009).
10. J. Yang, X.-y. Zhou, Y.-l. Zou, and J.-j. Tang, *Elect. Acta.,* 56, 8576-8581 (2011).
11. H. Wang, L.-F. Cui, Y. Yang, H. Sanchez Casalongue, J. T. Robinson, Y. Liang*, et al.*, *J. of the Amer. Chem. Soci.,* 132, 13978-13980 (2010).
12. H. Karim, M. A. I. Shuvo, M. T. Islam, G. Rodriguez, A. Sandoval, M. I. Nandasiri*, et al.*, *SPIE Smar. Stru. & Mate.+ Nond. Eval. & Heal. Moni.*, 94390I-94390I-6 (2015).
13. X. Zhu, Y. Zhu, S. Murali, M. D. Stoller, and R. S. Ruoff, *ACS nano.,* 5, 3333-3338 (2011).
14. Z.-S. Wu, W. Ren, L. Wen, L. Gao, J. Zhao, Z. Chen*, et al.*, *ACS nano.,* 4, 3187-3194 (2010).
15. Y. S. Hu, Y. G. Guo, R. Dominko, M. Gaberscek, J. Jamnik, and J. Maier, *Adv. Mat., 9,* 1963-1966 (2007).
16. W. Liu, L. Feng, C. Zhang, H. Yang, J. Guo, X. Liu*, et al.*, *J. of Mat. Chem. A,* 1, 6942-6948 (2013).
17. R.-J. Qi, Y.-J. Zhu, G.-F. Cheng, and Y.-H. Huang, *Nano.,* 16, 2502 (2005).

18. H. Pang and C. Chen, *RSC Adv.,* 4, 14872-14878 (2014).
19. N. Padmanathan and S. Selladurai, *RSC Adv.,* 4, 6527-6534 (2014).
20. C. Li, N. Sun, J. Ni, J. Wang, H. Chu, H. Zhou*, et al.*, *J. of Sol. Sta. Chem.,* 181, 2620-2625 (2008).
21. S. Maensiri, C. Masingboon, P. Laokul, W. Jareonboon, V. Promarak, P. L. Anderson*, et al.*, *Cry. grow. & des.,* 7, 950-955 (2007).
22. Z. Jamalzadeh, M. Haghighi, and N. Asgari, *Fro. of Env. Sci. & Eng.,* 7, 365-381 (2013).
23. L.-F. Cui, Y. Yang, C.-M. Hsu, and Y. Cui, *Nan. Let.,* 9, 3370-3374 (2009).
24. Q. Su, L. Chang, J. Zhang, G. Du, and B. Xu, *J. of Phy. Che. C,* 117, 4292-4298 (2013).
25. G. Wang, J. Bai, Y. Wang, Z. Ren, and J. Bai, *Scr. Mat.,* 65, 339-342 (2011).